

Table VII. Comparison of Experimental KIE with KIE Calculated from Model 3B, $A = 0.975$, for the Reaction of **1** with H_2 and D_2

temp, °C	k_H/k_D		
	exptl	calcd ^{a,c}	calcd ^{b,c}
0	1.170	1.218	1.164
5	1.147	1.202	1.143
10	1.140	1.186	1.124
20	1.125	1.158	1.088
25	1.107	1.144	1.071
30	1.072	1.132	1.056
$E_D - E_H$	0.406 ± 0.063	0.401	0.534
A_H/A_D	0.554 ± 0.062	0.581	0.435

^a $F_b = 0.1$; $n(\text{Ir-H}) = 0.7$. ^b $F_b = 0.2$; $n(\text{Ir-H}) = 0.5$. ^c Since the experiments and calculations did not employ identical sets of temperatures, these values are obtained from the Arrhenius parameters of the calculated values.

Table VIII. Summary of the Various Components of the Calculated KIE for the Reaction of **1** with H_2 and D_2 at 273 K, Transition State 3B, $A = 0.949$

$n(\text{Ir-H})$	F_b	MMI	EXC	ZPE	$(k_H/k_D)_s$	$Q_{\text{IH}}/Q_{\text{ID}}$	k_H/k_D
0.7	0.1	5.474	0.788	0.115	0.498	2.477	1.233
0.5	0.2	5.465	0.826	0.093	0.421	2.808	1.183

Figure 1 illustrates the experimental apparatus. In a typical run, 15.0 mL of a standard solution of **1** in toluene was injected by syringe into A. An equal amount of pure toluene was injected into A'. Each flask was equipped with a Teflon-coated stirring bar. A and A' were placed in a dry ice bath and subsequently evacuated to a pressure of 10^{-3} mmHg. The stopcock E was closed and each vessel allowed to warm to ambient

temperature. This freeze-thaw cycle was repeated three additional times, at which point both flasks were submerged in a constant temperature bath and the contents of each flask stirred vigorously. After a period of time sufficient to reach thermal equilibrium (15–30 min), hydrogen (deuterium) was simultaneously admitted to A and A' until a pressure of ca. 760 mmHg was reached. The stopcocks K and K' were then closed and data collection commenced.

Digitalization of the rate data was achieved by interfacing the analogue signal output from the MKS Model 170M-26A pressure meter through a Tecmar Lab Master A/D converter and subsequently to an IBM XT computer with use of the ASYST software system purchased from Macmillan Publishing Co. Pressure readings were recorded at intervals of 0.500 s (25–30 °C), 1.000 s (0–20 °C) and 2.000 s (<0 °C).

Registry No. **1**, 15318-31-7; H_2 , 1333-74-0; D_2 , 7782-39-0.

- (20) Muir, K. W.; Ibers, J. A. *J. Organomet. Chem.* **1969**, *18*, 175.
 (21) Chen, J.-Y.; Halpern, J.; Molin-Case, J. *J. Coord. Chem.* **1973**, *2*, 239.
 (22) Khare, G.; Eisenberg, R. *Inorg. Chem.* **1972**, *11*, 1385.
 (23) Bonnet, J.-J.; Jeannin, Y. *J. Inorg. Nucl. Chem.* **1973**, *35*, 4103.
 (24) Bird, P.; Harrod, J. F.; Than, K. A. *J. Am. Chem. Soc.* **1974**, *96*, 1222.
 (25) Shultz, A. J.; Khare, G.; McArdle, J. V.; Eisenberg, R. *J. Am. Chem. Soc.* **1973**, *95*, 3434.
 (26) Stancel, J. R.; Wellington, P. *Acta Crystallogr., Sect. A* **1969**, *25*, 5172.
 (27) Quiksall, C. O.; Spiro, T. G. *Inorg. Chem.* **1969**, *8*, 2011, 2363.
 (28) Nakamoto, K. "Infrared Spectra of Inorganic and Coordination Compounds;" Wiley: New York, 1970; pp 204–206.
 (29) Taylor, R. C.; Young, J. F.; Wilkinson, G. *Inorg. Chem.* **1966**, *5*, 20.
 (30) Muetterties, E. L., Ed. "Transition Metal Hydrides;" Dekker: New York, 1971; Chapters 3 and 4.
 (31) Adams, D. M. "Metal-Ligand and Related Vibrations;" St. Martins: New York, 1968; p 20.

Charge Carrier Trapping and Recombination Dynamics in Small Semiconductor Particles

Guido Rothenberger,[†] Jacques Moser,[†] Michael Grätzel,*[†] Nick Serpone,[‡] and Devendra K. Sharma[‡]

Contribution from the Institut de Chimie Physique, Ecole Polytechnique Fédérale, CH-1015 Lausanne, Switzerland, and the Chemistry Department, Concordia University, Montréal, Québec, Canada. Received July 31, 1985

Abstract: By using picosecond or nanosecond laser photolysis to excite colloidal (diameter 120 Å) particles of TiO_2 in aqueous solution, we have monitored the dynamics of charge carrier trapping and recombination in this semiconductor and interpret the results by a stochastic kinetic model. While the absorption spectrum of the trapped electron appears within the leading edge of the 30-ps laser pulse, the trapping of the hole is a much slower process requiring on the average 250 ns. At high electron-hole pair concentration in the particles, their recombination follows a second order law, the rate coefficient being $(3.2 \pm 1.4) \times 10^{-11} \text{ cm}^3 \text{ s}^{-1}$. Intraparticle recombination becomes first order at a very low charge carrier occupancy, the lifetime of a single electron-hole pair in a 120 Å sized TiO_2 particle being $(30 \pm 15) \text{ ns}$. Under these conditions, hole trapping, presumably by surface hydroxyl groups, competes with recombination and leads to a product whose reaction with trapped electrons is relatively slow. Implications for charge carrier mediated photoreactions are discussed.

Methods have recently been developed to produce stable dispersions of colloidal semiconductors with narrow size distribution. Due to their ultrafine size, these particles form transparent solutions which are amenable to analysis by laser photolysis technique.¹ So far studies have concentrated on interfacial charge transfer between the semiconductor and solution species or catalysts deposited on the semiconductor surface.² A microwave technique has been used to probe electronic processes in small particle suspensions.³ We apply here for the first time picosecond time-resolved spectroscopy to elucidate the dynamics of charge carrier reactions within the semiconductor particle. The systems

studied are 120 Å sized TiO_2 particles in aqueous solution. Photoinduced, charge carrier related processes in TiO_2 play a key

(1) (a) Duonghong, D.; Borgarello, E.; Grätzel, M. *J. Am. Chem. Soc.* **1981**, *103*, 4685. (b) Kalyanasundaram, K.; Borgarello, E.; Duonghong, D.; Grätzel, M. *Angew. Chem., Int. Ed. Engl.* **1981**, *20*, 987. (c) Duonghong, D.; Ramsden, J.; Grätzel, M. *J. Am. Chem. Soc.* **1982**, *104*, 2977. (d) Moser, J.; Grätzel, M. *Helv. Chim. Acta* **1982**, *65*, 1436. (e) Moser, J.; Grätzel, M. *J. Am. Chem. Soc.* **1983**, *105*, 6547.

(2) (a) Rossetti, R.; Brus, L. *J. Phys. Chem.* **1982**, *86*, 4470. (b) Rossetti, R.; Beck, S. M.; Brus, L. *J. Am. Chem. Soc.* **1982**, *104*, 7321. (c) Fox, M. A.; Lindig, B.; Chen, C. C. *J. Am. Chem. Soc.* **1982**, *104*, 5828. (d) Metcalfe, K.; Hester, R. E. *J. Chem. Soc., Chem. Commun.* **1983**, 133. (e) Chandrasekaran, K.; Thomas, J. K. *Chem. Phys. Lett.* **1983**, *97*, 357. (f) Henglein, A. *Ber. Bunsenges. Phys. Chem.* **1982**, *86*, 301. (g) Brown, G. T.; Darwent, J. R. *J. Phys. Chem.* **1984**, *88*, 4955. (h) Grätzel, M.; Moser, J. *Proc. Natl. Acad. Sci. U.S.A.* **1983**, *80*, 3129.

[†] Institut de Chimie Physique.

[‡] Concordia University.

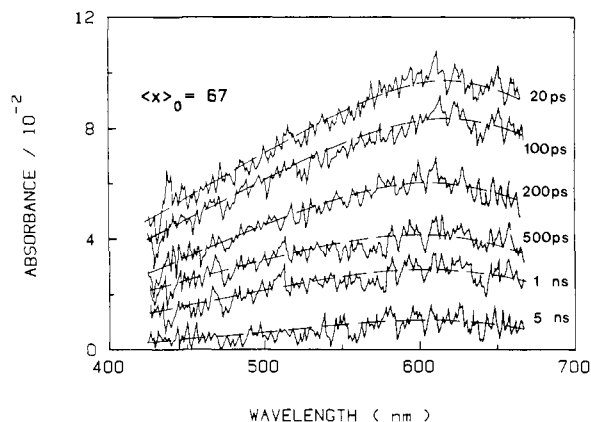


Figure 1. Transient spectra observed at various time intervals after picosecond excitation of colloidal TiO_2 . $[\text{TiO}_2] = 17 \text{ g/L}$, pH 2.7, solution deaerated with Ar, optical path length 0.2 cm. Average number of electron-hole pairs present initially in one TiO_2 particle is 67.

role in the degradation of paints,⁴ photocatalytic reactions,⁵ photography,⁶ and the conversion of light into chemical energy.⁷

Experimental Section

Colloidal solutions of TiO_2 (particle diameter 12 nm) were prepared and characterized as previously described.^{1d,e} All experiments were performed with unprotected sols in acidic aqueous solutions. Under these conditions, the colloid is stable for at least several weeks, and there is no growth in particle size.

The third harmonic (355 nm) of a double beam, passively mode-locked Nd-YAG laser was used to excite the particle. The pulse width at half height (fwhm) was 30 ps, and the energy per pulse was varied between 0.5 and 2 mJ. Details concerning the fast detection system used to monitor absorbance changes have been given elsewhere.⁸ Experiments where a small electron-hole pair concentration in the particles was desired were carried out with a Q-switched frequency-tripled Nd-YAG laser having a pulse width at half maximum of 15 ns.

Results

Figure 1 shows results obtained from the picosecond laser photolysis of aqueous TiO_2 solutions. The temporal evolution of the transient spectrum in the picosecond time domain is illustrated. The transient absorption observed after 20 ps⁹ exhibits a broad peak in the visible with a maximum around 620 nm. This is practically identical with the absorption spectrum of electrons produced in acidic (pH 3) TiO_2 sols by continuous illumination in the presence of hole scavengers.¹⁰ The appearance of a maximum in the visible indicates that at least part of the electrons are trapped. Very recent detailed EPR investigations have established that in acidic solutions the trapping sites are Ti^{4+} ions present at the particle surface.¹¹ From the fact that the electron spectrum is already fully developed at the end of the pulse, the trapping time is inferred to be less than 20 ps.

Under the conditions applied in Figure 1, the electron spectrum decays almost entirely in the picosecond time domain. A very small residual absorption appears to persist nevertheless even 5 ns after excitation of the particles. This contribution is too small to be assessed with certainty. The electron decay was found to

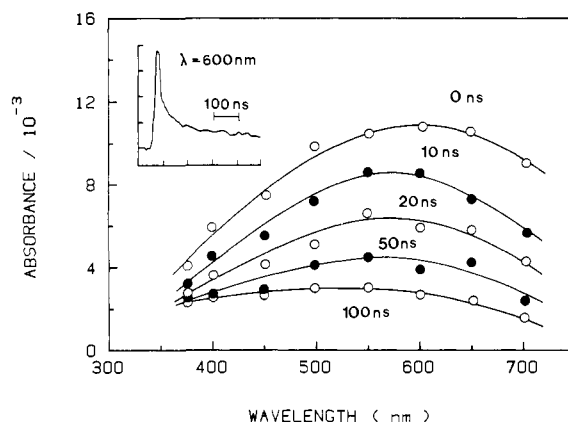


Figure 2. Transient spectra observed at various time intervals after excitation of colloidal TiO_2 particles with a 15-ns pulse of a frequency-tripled Nd laser. $[\text{TiO}_2] = 5 \text{ g/L}$, pH 2.7, solution deaerated with Ar, optical path length 0.5 cm. Average number of electron-hole pairs present initially in one TiO_2 particle is six. Inserted oscillogram shows formation and decay of the electron absorption at 600 nm.

obey a second-order rate law, and a detailed kinetic analysis of this process will be given below. Note that there are no significant spectral changes during the decay reaction. The spectra monitored at different time intervals after the laser pulse exhibit essentially the same features, the maximum of the transient absorbance remaining at 620 nm.

As would be expected for a second-order kinetic process, the rate at which the transient spectrum relaxes was found to depend on the number of electron-hole pairs present initially in a particle, which in turn depends on the fluence of the exciting pulse. The higher the initial number of pairs, the faster was the relaxation. In Figure 1, the number of $e^- - h^+$ pairs present 20 ps after the pulse maximum is 67 based on an extinction coefficient of $1200 \text{ M}^{-1} \text{ cm}^{-1}$ for the electron absorption at 600 nm.¹⁰ Experiments were carried out also at higher fluences producing an initial $e^- - h^+$ pair concentration of up to 300/particle. No change in the shape of the transient spectrum was noticed, only the relaxation was faster. The half-lifetime for the electron decay was found to be inversely proportional to the number of electron-hole pairs initially present in the particles under these conditions.

A series of experiments was also carried out at low laser fluence where the initial number of $e^- - h^+$ pairs generated in the colloidal TiO_2 particles was below ten. Here, the electron-hole recombination becomes visible on a nanosecond time scale. However, since the transient absorbance is small, a more sensitive detection system was employed in conjunction with 15-ns laser excitation.

Figure 2 shows results obtained from the laser photolysis of colloidal TiO_2 solutions where six electron-hole pairs were initially present in each particle. The transient spectra obtained are very similar to those displayed in Figure 1. However, the decay of the absorption occurs here in a much slower fashion. Even after 100 ns a significant fraction of the absorption remains. The ratio of initial transient absorbance to that present in the plateau region after completion of the fast decay was found to increase with increasing electron-hole pair concentration in the particles. The spectrum after 100 ns appears to be blue shifted with respect to the one obtained immediately after the laser pulse. Thus, at 400 nm the ratio of the absorbance measured immediately and 100 ns after the laser pulse is close to two, while it exceeds five in the red part of the spectrum. This point will be further discussed below.

Inserted in Figure 2 is an oscilloscope trace illustrating the temporal behavior of the 600-nm absorption. The signal appears within the leading edge of the laser pulse and decays thereafter very rapidly until a plateau is reached from where on further decay is comparatively slow.

Laser excitation of colloidal TiO_2 with the lowest possible fluence compatible with the noise of the signal was attempted to decrease further the $e^- - h^+$ pair concentration. Figure 3 shows the decay of the 800-nm absorption under conditions where only

(3) Warman, J. M.; de Haas, M. P.; Grätzel, M.; Infelta, P. P. *Nature (London)* **1984**, *310*, 305.

(4) Völz, H. G.; Kämpf, G.; Fitzky, H. G. *Farbe Lack* **1972**, *78*, 1037.

(5) (a) Bard, A. J. *J. Photochem.* **1979**, *10*, 59. (b) Bard, A. J. *J. Phys. Chem.* **1982**, *86*, 172.

(6) Addis, R. R.; Wakim, F. G. *Photogr. Sci. Eng.* **1969**, *13*, 111.

(7) Grätzel, M., Ed. "Energy Conversion Through Photochemistry and Catalysis"; Academic Press: New York, 1983.

(8) Ponterini, G.; Serpone, N.; Bergkamp, M. A.; Netzel, T. L. *J. Am. Chem. Soc.* **1983**, *105*, 4639.

(9) The time zero is taken as the time of maximum overlap of the probe and pump pulses. In the present case, this corresponds to approximately the time when half of the integral intensity of the excitation pulse has been absorbed.

(10) Kölle, U.; Moser, J.; Grätzel, M. *Inorg. Chem.* **1985**, *24*, 2253.

(11) Howe, R.; Grätzel, M. *J. Phys. Chem.* **1985**, *89*, 4495.

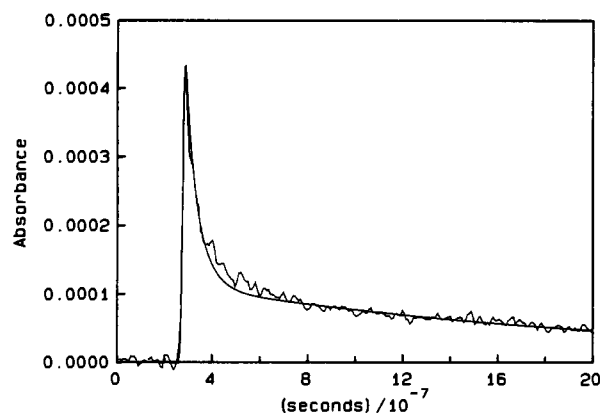
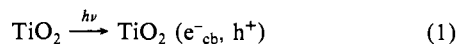


Figure 3. Transient absorbance observed at 800 nm. $[\text{TiO}_2] = 5 \text{ g/L}$, pH 3.0, solution deaerated with Ar, optical path length = 0.5 cm. The noisy curve is an average of 30 single shot curves. The full line is calculated via the integration of eq 15. The parameters used were $\langle x \rangle_0 = 0.85$, $k = 1.3 \times 10^7 \text{ s}^{-1}$, $k_1 = 4 \times 10^6 \text{ s}^{-1}$, $k_2 = 5.5 \times 10^5 \text{ s}^{-1}$. Average number of electron-hole pair derived from the maximum deflection of the signal after the laser pulse is 0.65. The parameter $\langle x \rangle_0 = 0.85$ corresponds to the number of electron-hole pairs that would have been obtained if the reactions that cause the disappearance of electrons and holes were infinitely slow.

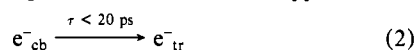
0.85 charge carrier pairs per particle were created by the laser pulse.¹² The experimental curve is an average of 30 single shots recorded on two different time scales by a transient digitizer. The solid line drawn through this curve is a computer fit to a kinetic model which will be discussed in the following section.

Discussion

In the present study, a short laser pulse was used to produce electron-hole pairs in colloidal TiO_2 particles. The characteristic



optical absorption of trapped electrons in these semiconductor particles was used to analyze their formation and decay kinetics. It was found that the spectrum of the trapped electrons developed within the leading edge of the picosecond laser pulse. This sets the upper limit for the average time of electron trapping at 20 ps. Since in acidic TiO_2 sols the electrons are trapped at Ti^{4+}

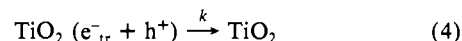


sites located at the particle-water interface,¹¹ the relaxation into the trap is preceded by diffusion of conduction band electrons to the particle surface. For randomly generated charge carriers the average diffusion time from the bulk to the surface is given by¹³

$$\tau = r^2 / \pi^2 D \quad (3)$$

where r is the particle radius and D the diffusion coefficient of the carrier. The diffusion coefficient of conduction band electrons in TiO_2 , due to their heavy effective electron mass ($m_{\text{eff}} = 30 \times m_e$ ¹⁴), is relatively small, $D_{e^-} = 2 \times 10^{-2} \text{ cm}^2/\text{s}$. Nevertheless, eq 3 predicts an average transit time of only 1.8 ps for 120 Å sized TiO_2 particles. If an electrical field is present in the semiconductor, the transit time could be further reduced as has been pointed out by Albery and Bartlett.¹⁵ Our experimental observations confirm that both the diffusion of conduction band electrons from the particle interior to the interface as well as their subsequent relaxation into the trapping surface states is a very rapid process. By contrast, we have no evidence for efficient hole trapping in the picosecond time domain. The transient spectrum in Figure 1 is identical with that of trapped electrons obtained by steady-state illumination of colloidal TiO_2 in the presence of hole scavengers.¹⁰

Bahnemann et al.¹⁶ have published a spectrum with a maximum around 450 nm which they attribute to valence band holes trapped by surface hydroxyl groups of colloidal TiO_2 . In Figure 1, we failed to observe the formation of such an absorption. Thus, either the hole trapping occurs on a time scale longer than picosecond or the extinction coefficient of the trapped hole is much smaller than that of the electron. The first proposition is more realistic (vide infra), and we assume in the following that the recombination reaction observed at higher laser fluence on the picosecond time scale involves trapped electrons and free valence band holes. We shall discuss the participation of trapped holes in the $e^- - h^+$ recombination below in connection with the nanosecond laser results.



A particularly important aspect of reaction 4 is that it involves a very limited amount of electron-hole pairs confined to the minute reaction space of a 120 Å sized TiO_2 particle. This renders necessary a stochastic approach in the interpretation of the results. Furthermore, the generation of electron-hole pairs during the light reaction is a statistic process. Therefore, the number of electron-hole pairs generated by the laser is not the same in every particle, but rather follows a statistical distribution. In the following, we shall develop a kinetic model in which these crucial points are taken into account.

(i) Statistical Distribution of Electron-Hole Pairs among the Semiconductor Particles. The statistical law that governs the distribution of electron-hole pairs over the semiconductor particles at the end of the laser pulse will be derived first. We shall assume that the duration of the pulse is much shorter than the time period over which the charge carriers decay, i.e., we suppose that excitation of the particles is a δ function. This condition will be dropped later in the interpretation of the ns laser data where it is not applicable. For convenience, we consider the semiconductor particles as spheres of uniform size. Thus, in the spherical TiO_2 aggregates of 60-Å radius which were investigated here, there are 2.6×10^4 Ti atoms per particle. A parameter of interest is the maximum number of electron-hole pairs that can be produced in a particle (m). This number is determined by the density of electronic states n_c available in the conduction band of the semiconductor. For TiO_2 , $n_c \approx 5 \times 10^{21} \text{ cm}^{-3}$, which gives 3600 states/particle, and hence $m \approx 3600$. Let n be the number of particles per unit volume. Then $M = nm$ is the maximal number of pairs that could exist in a unit volume. Suppose that the number of pairs that are actually observed in this volume immediately after the laser pulse is M^* . Then, we have

$$a = M^* / M \quad (5)$$

where a is the probability that one of the m possible transitions is actually excited. The average number of pairs per particle immediately after the laser pulse is

$$\langle x \rangle_0 = \frac{M^*}{n} = a \cdot \frac{M}{n} = am \quad (6)$$

The probability $B(x, m, a)$ that a semiconductor particle contains x electron-hole pairs after excitation depends on m , the maximum possible number of pairs, as well as on a . B can be expressed as the product of the probability a^x that a group of x transitions is excited times the probability $(1 - a)^{m-x}$ that the remaining $m - x$ transitions are not excited times the number of distinct ways of selecting x transitions from an initial group of m .

$$B(x, m, a) = \frac{m!}{x! (m-x)!} a^x (1-a)^{m-x} \quad (7)$$

This Bernoulli distribution reduces to a Poisson distribution¹⁷ for large m and $a \ll 1$, i.e., conditions which are satisfied in the experiments to be analyzed. Therefore, we shall apply in the following the Poisson equation

(12) The extinction coefficient for the trapped electron in acidic TiO_2 sols is $780 \text{ M}^{-1} \text{ cm}^{-1}$ at 800 nm.

(13) Grätzel, M.; Frank, A. *J. Phys. Chem.* **1982**, *86*, 2964.

(14) (a) Breckenridge, R. G.; Hosler, W. R. *Phys. Rev.* **1953**, *91*, 793. (b) Yania, Y. *Ibid.* **1963**, *130*, 1711.

(15) Albery, W. J.; Bartlett, P. N. *J. Electrochem. Soc.* **1984**, *131*, 315.

(16) Bahnemann, D.; Henglein, A.; Lilie, J.; Spanhel, L. *J. Phys. Chem.* **1984**, *88*, 709.

(17) Chandrasekhar, S. *Rev. Mod. Phys.* **1943**, *15*, 1.

$$P(x, \langle x \rangle_0) = \frac{\langle x \rangle_0^x}{x!} \exp(-\langle x \rangle_0) \quad (8)$$

to derive the distribution of electron-hole pairs among the semiconductor particles following laser excitation.

(ii) **Time Law for the Kinetics of Electron-Hole Recombination in a Small Semiconductor Particle.** The general kinetic features of reactions involving a small number of reactants in confined space have previously been explored by McQuarrie,¹⁸ and we apply now these concepts to the specific case of electron-hole recombination in semiconductor particles. A precise rate equation will be derived, and it will be shown that the conventional first- and second-order rate laws applied in homogeneous solution kinetics will emerge as limiting cases for single and very high occupancy of the semiconductor particles by electron-hole pairs, respectively. It is assumed that the charge carriers undergo random and independent diffusion in the particles. For TiO₂, this is a reasonable assumption since due to the heavy mass of the charge carriers, their Bohr radius is small (for free conduction band electrons in TiO₂ $r_{\text{Bohr}} \approx 2 \text{ \AA}$). In the trapped state the electron is confined to a titanium ion site at the surface of the particle. Furthermore, the Coulombic attraction between electrons and holes is shielded due to the high dielectric constant ($\epsilon = 130$) of this semiconductor. In such a case, the recombination kinetics can be modeled by a quadratic birth and death process which implies that the survival probability of a single electron-hole pair in a semiconductor particle decreases exponentially with time, the average lifetime being $\tau = k^{-1}$. If x pairs are present in a particle, the first recombination event yielding a particle with $(x - 1)$ pairs will occur after an average time of $\tau = (x^2 k)^{-1}$. The factor x^2 allows for the fact that x^2 different choices can be made from an ensemble of x electrons and x holes. The time differential of the probability that a particle contains x electron-hole pairs at time t is given by

$$dP_x(t)/dt = k(x + 1)^2 P_{x+1}(t) - kx^2 P_x(t) \quad (9)$$

where $x = 0, 1, 2, 3 \dots$

This system of differential equations is to be solved subject to the initial conditions (8) for $P_x(0)$, i.e., the Poisson distribution law. The average number of pairs present at time t , $\langle x \rangle(t)$, can be calculated by means of the generating function technique^{18,19} yielding

$$\langle x \rangle(t) = \sum_{n=1}^{\infty} c_n \exp(-n^2 kt) \quad (10)$$

where

$$c_n = 2 \exp(-\langle x \rangle_0) (-1)^n \sum_{i=n}^{\infty} \frac{\langle x \rangle_0^i}{(n+i)!} \prod_{j=1}^n (n-i-j) \quad (11)$$

The parameter $\langle x \rangle_0$ is the average number of pairs present at $t = 0$.

Two limiting cases of eq 10 are particularly relevant: When $\langle x \rangle_0$ is very small, eq 10 becomes a simple exponential and the electron-hole recombination follows a first-order rate law. Conversely, at high average initial occupancy of the semiconductor particles by electron-hole pairs, eq 10 approximates to a second-order rate equation

$$\langle x \rangle(t) = \frac{\langle x \rangle_0}{1 + \langle x \rangle_0 kt} \quad (12)$$

The domain of validity of these approximations is quantitatively assessed in Figure 4 where the product $\langle x \rangle_0 k \tau_i$ ($i = 1/2, 1/4, 1/8$), calculated from eq 10, is plotted as a function of $\langle x \rangle_0$. The parameters $\tau_{1/2}$, $\tau_{1/4}$, and $\tau_{1/8}$ correspond to 1, 2, and 3 half-lives, respectively, i.e., the times at which $1/2$, $1/4$, and $1/8$ of the pairs present initially still survive. For a first-order process $\langle x \rangle_0 k \tau_i = -\ln(i) \langle x \rangle_0$. This limit is represented by the three

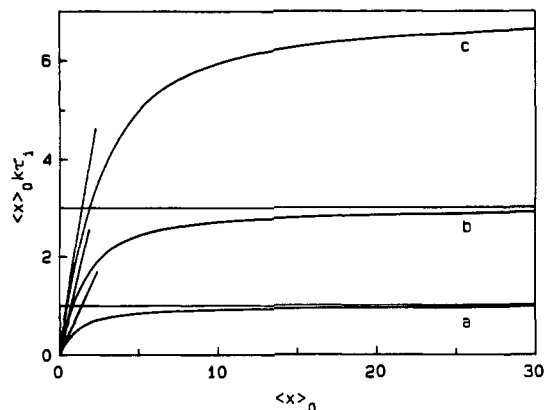


Figure 4. $\langle x \rangle_0 k \tau_i$ vs. $\langle x \rangle_0$ for $i = 1/2$ (a); $i = 1/4$ (b); $i = 1/8$ (c). The full lines are calculated (eq 10). The straight lines which pass through the origin correspond to the first-order approximation, and the horizontal lines at ordinates 1, 3, and 7 correspond to the second-order approximation.

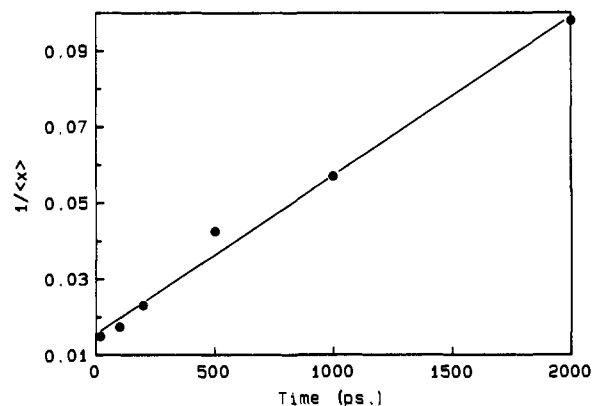


Figure 5. $\langle x \rangle^{-1}$ vs. time calculated from the absorbancies at 600 nm of Figure 1. The straight line corresponds to the second-order kinetics of eq 12.

straight lines which pass through the origin. On the other hand, for a second-order process $\langle x \rangle_0 k \tau_i = (1/i) - 1$. This limit is represented by the three horizontal lines at ordinate values of 1, 3, and 7 in Figure 4. From this presentation, one concludes that a first-order approximation is unsatisfactory already at $\langle x \rangle_0 = 0.5$, whereas a second-order rate law is a good approximation for $\langle x \rangle_0$ larger than about 30. We notice also that the approximations are best at short times.

(iii) **Intraparticle Electron-Hole Recombination at High Charge Carrier Concentration, Analysis of Picosecond Time-Resolved Experiments.** In these experiments the average number of electron-hole pairs present after the laser pulse was varied between 60 and 300. In agreement with the prediction of eq 10 and Figure 4, the kinetic evaluation shows that the second-order rate eq 12 represents satisfactorily the decay of the electron absorption up to a time corresponding to $\tau_{1/8}$. As an example, we plot in Figure 5 $\langle x \rangle^{-1}(t)$ as a function of time using the experimental data from Figure 1. A linear relation is obtained, and using a least-squares fit to the straight line, one derives a rate constant of $k = (4.2 \pm 0.2) \times 10^7 \text{ s}^{-1}$. The average rate constant determined from four different $\langle x \rangle_0$ values between 67 and 300 is $k = (3.5 \pm 1.5) \times 10^7 \text{ s}^{-1}$, corresponding to a mean lifetime for a single electron-hole pair in a colloidal TiO₂ particle of $30 \pm 15 \text{ ns}$. No systematic trend of k with $\langle x \rangle_0$ was observed.

(iv) **Intraparticle Electron-Hole Recombination at Low Charge Carrier Concentration, Analysis of Nanosecond Time-Resolved Experiments.** The simplified model used in the previous section is not suited to analyze the data displayed in Figures 2 and 3. First, $\langle x \rangle_0$ being small, the second-order approximation does not hold, and the full stochastic set of eq 10 should be used. Second, even if eq 10 were used, the experimental data could not be fitted correctly. It is apparent from Figures 2 and 3 that the electron

(18) (a) McQuarrie, D. A. *J. Appl. Prob.* 1967, 4, 413. (b) McQuarrie, D. A. *Adv. Chem. Phys.* 1969, 15, 149.

(19) Feller, W. "An Introduction to Probability Theory and its Applications"; John Wiley and Sons: New York, 1971; Vol. 1.

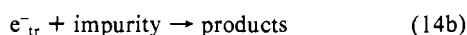
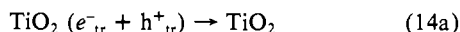
absorption decays in two steps. A first and rapid decrease leads to a plateau from where further decay is slow on the time scale employed. This distinguishes the results obtained at low $\langle x \rangle_0$ from those at high electron-hole concentration (Figure 1) where the residual absorption after completion of the fast electron decay is very small. Third, in the low fluence experiments, a 15 ns fwhm laser pulse was used to excite the semiconductor particles. The pulse width is comparable to the time period during which the fast electron decay takes place rendering the assumption of δ function excitation unrealistic.

The appearance of a plateau in the decay curve of the electron absorption indicates a process competing with reaction 4 during which the complementary charge carriers, i.e., the valence band holes, are trapped



Apparently, in the trapped state the hole is much less reactive toward e^-_{tr} than when it moves freely in the valence band. The detailed nature of the trapped hole state cannot be assessed with certainty from the present study. Bahnemann et al. conclude from flash photolysis studies of colloidal TiO_2 in the presence of Pt that the surface trapped hole, i.e., $>Ti-O^+$, has an absorption maximum at 450 nm. On the other hand, King and Freund²⁰ have recently obtained unambiguous evidence that trapped hole states in oxides undergo very efficient dimerization forming μ -peroxides. In our recent EPR investigations with colloidal TiO_2 , we failed to detect, even at 4 K, the formation of paramagnetic centers under illumination which could be ascribed to the trapped hole.¹¹ There is no doubt, on the other hand, that surface bound peroxides are formed during the steady state irradiation of TiO_2 sols.²¹ These observations would favor the assignment of the trapped-hole state to peroxides. The spectra in Figure 2 seems to show a shift of the transient absorption to shorter wavelength as the recombination reaction proceeds. Unfortunately, the weakness of the signal at longer times prevents us from assessing with certainty the features of the underlying absorption which overlaps with the electron spectrum.

The slow decay of the electron absorption in Figures 2 and 3 is attributed to the reaction of electrons with trapped holes or reducible impurities, such as oxygen



Note that although reaction 14a is a bimolecular process, it is expected from eq 10 to follow first-order kinetics when, on average, much less than one electron-hole pair per particle is present after the fast recombination. This condition is fulfilled in Figure 3 where the electron concentration after completion of the rapid part of the absorption decay is 0.17/particle. In the following analysis, we assume, therefore, that the slow electron decay obeys an exponential time law, the rate parameter k_2 representing the sum of the rate constants for reactions 14a and 14b. The master equations which describe the temporal evolution of the system are the following:

$$dP_{x,y}(t)/dt = G_{x,y}(t) + k(x+1)(y+1)P_{x+1,y+1}(t) + k_1(x+1)P_{x+1,y}(t) + k_2(y+1)P_{x,y+1}(t) - (kxy + k_1x + k_2y)P_{x,y}(t) \quad (15)$$

where $x = 0, 1, 2, \dots$; $y = 0, 1, 2, \dots$

Here, $P_{x,y}(t)$ is the probability that a particle contains x holes and y electrons at time t . The function $G_{x,y}(t)$ describes the rate of electron-hole pair generation during the laser pulse. Details concerning the evaluation of this term are given in the appendix. The system of differential eq 15 was numerically integrated with a modified Runge-Kutta method.²² Knowing $P_{x,y}(t)$, the electron

concentration and the time profile of the transient absorption at 800 nm are readily calculated. In eq 15, there are four independently adjustable parameters: $\langle x \rangle_0$ and the rate constants k , k_1 , and k_2 . Here, the variable $\langle x \rangle_0$, which is contained in $G_{x,y}(t)$, is the total average number of pairs produced by the laser pulse which would have been measured after the light flash if the three rate constants were equal to zero. These four parameters were varied until a satisfactory agreement with the data depicted in Figure 3 was found. $\langle x \rangle_0$ determines mainly the initial height of the signal, k the decay at short time, k_1 the height of the plateau, and k_2 the absorption decrease at long time. The full line in Figure 3 represents the optimal fit obtained with the parameters $\langle x \rangle_0 = 0.85$, $k = 1.3 \times 10^7 \text{ s}^{-1}$, $k_1 = 4 \times 10^6 \text{ s}^{-1}$, and $k_2 = 5.5 \times 10^5 \text{ s}^{-1}$. Changing these parameters by 10% leads to a fit which is significantly worse.

The rate coefficient for electron-hole recombination derived from Figure 3 is somewhat smaller than the value of $(3.5 \pm 1.5) \times 10^7 \text{ s}^{-1}$ obtained from the picosecond experiments where the charge carrier density was high. However, in view of the experimental error affecting the ps kinetics and the limited time response of the ns detection system, the agreement is surprisingly good.

From eq 15 it is expected that for a given set of rate constants the fraction of electrons which do not undergo fast recombination with valence band holes is expected to decrease with increasing $\langle x \rangle_0$. This explains why at high initial electron-hole pair concentration, i.e., conditions fulfilled in Figures 1 and 5, practically all charge carriers recombine rapidly, and the final absorbance is negligibly small.

Since the volume of a 60 Å radius TiO_2 particle is $9 \times 10^{-19} \text{ cm}^3$, the bulk rate constant for carrier recombination, $k_r = V_{\text{particle}}k$, is $(3.2 \pm 1.4) \times 10^{-11} \text{ cm}^3 \text{ s}^{-1}$. This is about 300 times smaller than the rate coefficient for carrier recombination via defects in silicon for which a value of $10^{-9} \text{ cm}^3 \text{ s}^{-1}$ has been derived.²³

It is instructive to compare our results to the kinetic data obtained recently by Brown and Darwent from the steady-state photolysis of colloidal TiO_2 solutions in the presence of methyl orange and oxygen as electron scavengers.²⁸ From the quantum yield of product formation, the ratio of the rate constant for electron-hole recombination to that for hole trapping was evaluated as 450. Assuming that the recombination coefficient in their material was also $3.2 \times 10^{-11} \text{ cm}^3 \text{ s}^{-1}$ and taking into account that their particles were n -doped with an electron density of $n_e = 1 \times 10^{19} \text{ cm}^{-3}$, the value for the pseudo-first-order constant for electron-hole recombination, $k'_r = k_r \times n_e$, is $3.2 \times 10^8 \text{ s}^{-1}$. By using for the hole trapping rate our value, i.e., $k_1 = 4 \times 10^6 \text{ s}^{-1}$, k'_r/k_1 is predicted to be 80, which is of the same order of magnitude as the ratio of 450 determined experimentally by Brown and Darwent.²⁸ Presumably, the difference in the two values arises from the fact that the TiO_2 particles employed by Brown and Darwent are larger ($r = 330 \text{ Å}$) than ours.

Conclusions

By using picosecond and nanosecond laser photolysis to excite colloidal TiO_2 particles of 60-Å radius in aqueous solution, we have been able to obtain important information on the dynamics of charge carrier trapping and recombination in this semiconductor material. The trapping of conduction band electrons was shown to be a very rapid process occurring within the leading edge of the 30-ps laser flash. By contrast, the trapping of the valence band hole, presumably by surface OH^- groups, is a much slower process requiring an average time of 250 ns.

Taking advantage of the characteristic optical absorption of trapped electrons in the colloidal TiO_2 particles, we have recorded their recombination with free and trapped holes in the 10^{-11} to 10^{-6} s time domain. We have furthermore conceived a stochastic kinetic model to interpret these observations. If the initial electron-hole pair concentration in the particles is high, i.e., >60 , their recombination follows second-order kinetics. Under these conditions, practically all the charge carriers recombine within a

(20) King, B. V.; Freund, F. *Phys. Rev. B* **1984**, *29*, 5814.

(21) Duonghong, D.; Grätzel, M. *J. Chem. Soc., Chem. Commun.* **1984**, 1597.

(22) Ralston, A.; Wilf, H. S. "Mathematical Methods for Digital Computers"; John Wiley and Sons: New York, 1960; Vol. 1.

(23) Landsberg, P. T.; Konsik, G. S. *J. Appl. Phys.* **1984**, *56*, 1696.

nanosecond. The recombination coefficient between trapped electrons and free holes was determined as $3.2 \times 10^{-11} \text{ cm}^3 \text{ s}^{-1}$. At very low occupancy of the semiconductor particles by electron-hole pairs, their recombination becomes first order, the mean lifetime of a single electron-hole pair being 30 ns. Under these conditions hole trapping can compete with charge carrier recombination. In the trapped state, the hole is relatively unreactive toward electrons which survive in the particles for many microseconds.

These results elucidate earlier findings obtained from the study of interfacial electron transfer from colloidal TiO_2 particles to acceptors such as methylviologen. In acid solution, the charge transfer occurred in the 10^{-6} to 10^{-3} s domain indicating the presence of long-lived electrons in the semiconductor particles, even in the absence of hole scavengers. Hole trapping by hydroxide groups at the particle surface (eq 13) leading to a product whose reaction with electrons is relatively slow provides a rationale for these observations.

With regard to the use of colloidal TiO_2 as a photocatalyst for the light-induced cleavage of water, the fact that recombination of electrons with free holes is about 10 times faster than hole trapping is disadvantageous. This explains why highly active catalysts are required to accelerate the charge carrier reactions with water. We agree with the conclusion of Brown and Darwent that fast removal of holes from the TiO_2 particle is particularly important to avoid recombination.²⁸ Catalysts such as RuO_2 deposited onto the particle surface can serve this purpose since they act as hole transfer catalysts.^{1c,d} Enhancement of hole transfer to water is likely to be the reason for the beneficial effect RuO_2 exerts on the quantum yield of water decomposition.^{1a,24,25}

Work is presently in progress to assess in which way the rate of charge carrier recombination and trapping is affected by external parameters such as pH and temperature as well as the internal structure and composition of the semiconductor particles. Preliminary studies show that the rate of electron-hole recombination can be drastically accelerated or retarded by doping the colloidal particles with suitable transition-metal ions. A report on these results is forthcoming.

Appendix

The generation term $G_{x,y}(t)$ is the rate at which the probability $P_{x,y}(t)$ changes as a result of the creation of electron-hole pairs

- (24) Kawai, T.; Sakata, T. *Nature (London)* **1980**, *286*, 474.
 (25) Blondeel, G.; Harriman, A.; Williams, D. *Solar Energy Mater.* **1983**, *9*, 217.

by the laser pulse. $G_{x,y}(t)$ was calculated in the following way: suppose that at time t we have the probability distribution $P_{x,y}(t)$. During a time interval Δt , the laser pulse creates on the average $\Delta n(t, \Delta t)$ pairs per particle, with

$$\frac{\Delta n(t, \Delta t)}{\Delta t} = \frac{\langle x \rangle_0}{(2\pi)^{1/2} \sigma} e^{-(t-t_0)^2/2\sigma^2} \quad (\text{A1})$$

Here, we have assumed that the temporal profile of the laser pulse is a Gaussian. The parameter σ is determined by recording the scatter of the laser pulse with a transient digitizer; $\langle x \rangle_0$, an adjustable parameter, is the average number of electron-hole pairs per particle that the laser pulse creates. The parameter t_0 has to be chosen large enough so that an integration starting from time $t = 0$ includes more than 99.9% of the area under the Gaussian.

According to eq 8, these $\Delta n(t, \Delta t)$ pairs will be distributed over the particles according to a Poisson distribution

$$Q_{x,y}(t, \Delta t) = \delta_{x,y} \frac{\Delta n(t, \Delta t)^x}{x!} e^{-\Delta n(t, \Delta t)} \quad (\text{A2})$$

where $\delta_{x,y}$ implies that an equal number of electrons and holes are created.

The electron-hole distribution at time $t + \Delta t$ will be the combination of the distribution $P_{x,y}(t)$ describing the system at time t and of $Q_{x,y}(t, \Delta t)$ which is the distribution of the pairs added to the system between t and $t + \Delta t$.

$$P_{x,y}(t + \Delta t) = \sum_{a=0}^x \sum_{b=0}^y P_{a,b}(t) Q_{x-a,y-b}(t, \Delta t) \quad (\text{A3})$$

Finally, $G_{x,y}(t)$ is calculated by using the definition of a derivative:

$$G_{x,y}(t) = \lim_{\Delta t \rightarrow 0} \frac{P_{x,y}(t + \Delta t) - P_{x,y}(t)}{\Delta t} \quad (\text{A4})$$

In practice, Δt was chosen small enough so as to ensure a good accuracy on the numerical determination of $G_{x,y}(t)$.

Acknowledgment. This work was supported by the Swiss National Science Foundation and the Gas Research Institute, Chicago, IL (subcontract with the Solar Energy Research Institute, Golden, Colorado). N.S. thanks the Natural Sciences and Engineering Research Council of Canada for support. We enjoyed helpful discussions with Dr. P. P. Infelta during the course of this work.

Distonic Oxonium and Ammonium Radical Cations. A Neutralization–Reionization and Collisional Activation Study

Chrysostomos Wesdemiotis, Paul O. Danis, Rong Feng, Jacqueline Tso, and Fred W. McLafferty*

Contribution from the Chemistry Department, Cornell University, Ithaca, New York 14853.
 Received April 15, 1985

Abstract: The distonic radical ions $\cdot\text{CH}_2\text{CH}_2\text{X}^+\text{H}$, $\cdot\text{CH}_2\text{CH}_2\text{CH}_2\text{X}^+\text{H}$, $\cdot\text{CH}_2\text{CH}(\text{CH}_3)\text{CH}_2\text{X}^+\text{H}$, and $\cdot\text{CH}_2\text{CH}_2\text{CH}_2\text{CH}_2\text{X}^+\text{H}$, where $\text{X} = \text{OH}$ or NH_2 , and their molecular ion counterparts HRX^+ have been studied with isotopic labeling and mass spectra produced by neutralization–reionization (NR) and collisionally activated dissociation (CAD). The isomerization $\text{HRX}^+ \rightarrow \cdot\text{RX}^+\text{H}$ is more exothermic for $\text{X} = \text{OH}$, but has a lower activation energy for $\text{X} = \text{NH}_2$. For this reaction a 1,5-hydrogen rearrangement is favored over 1,4-H, and the 1,3-H and 1,2-H rearrangements were not observed. NR spectra are particularly valuable for characterizing the distonic $\cdot\text{RX}^+\text{H}$ ions, as neutralization produces an unstable hypervalent species. CAD spectra of larger $\cdot\text{RX}^+\text{H}$ and HRX^+ ions are very similar; activation of $\cdot\text{RN}^+\text{H}_3$ mainly causes isomerization to HRNH_2^+ , which dissociates by α -cleavage, the lowest energy pathway.

Removal of an electron from a gaseous molecule yields an odd-electron molecular ion whose charge and radical centers are

ostensibly at the same site, e.g., ionized butanoic acid (1) and 1-butanol (4). Distonic radical ions,^{1,2} in which the radical and